COMMUNICATION

Micropatterning and Functionalization of Single Layer Graphene: Tuning Its Electron Transport Properties

Miao-Miao Cui [a], Lian-Huan Han [a,b,*], Lan-Ping Zeng [a], Jia-Yao Guo [a], Wei-Ying Song [a], Chuan Liu [a], Yuan-Fei Wu [a], Shi-Yi Luo [a], Yun-Hua Liu [c,*], Dong-Ping Zhan [a,*]

[a] Department of Chemistry, College of Chemistry and Chemical Engineering, State Key Laboratory of Physical Chemistry of Solid Surfaces (PCOSS), Engineering Research Center of Electrochemical Technologies of Ministry of Education, Xiamen University, Xiamen 361005, China
[b] Department of Mechanical and Electrical Engineering, Pen-Tung Sah Institute of Micro-Nano Science and Technology, Xiamen University, Xiamen 361005, China
[c] National CAD Support Software Engineering Research Center Huazhong University of Science and Technology, Wuhan 430074, China

Abstract

As a promising 2D material, graphene exhibits excellent physical properties including single-atom-scale thickness and remarkably high charge carrier mobility. However, its semi-metallic nature with a zero bandgap poses challenges for its application in high-performance field-effect transistors (FETs). In order to overcome these limitations, various approaches have been explored to modulate graphene's bandgap, including nanoscale confinement, external field induction, doping, and chemical micropatterning. Nevertheless, the stability and controllability still need to be improved. In this study, we propose a feasible method that combines electrochemical bromination and photolithography to precisely tune the electron transport properties of single layer graphene (SLG). Through this method, we successfully fabricated various brominated SLG (SLGBr) micropatterns with high accuracy. Futher investigation revealed that the electron transport properties of SLG can be conveniently tuned by controlling the degree of bromination. The SLGBr exhibited a resistance, and have a decreasing conductance with the bromination degree increasing. When the bromination degree increased to a critical value, the SLGBr demonstrated semiconducting characteristics. This research offers a prospective route for the fabrication of graphene-based devices, providing potential applications in the realm of microelectronics.

Keywords: Graphene patterning; Electron transport; Electrochemical bromination; Photolithography; All graphene device

1. Introduction

Graphene has been considered as the most prospective material because of its excellent properties, including single-atom-scale thickness [1], extremely high charge carrier mobility [2], superior optical transparency [3], high thermal conductivity [4], etc. Recently, the mass production of high-quality single layer graphene (SLG) at wafer scale makes it qualified in various possible applications such as micro/nano-electronics, sensors and actuators, microelectromechanical system (MEMS), etc. [5—7]. To this, the localized micropatterning and functionalization of SLG at wafer scale are crucial in order to tune the physical and chemical properties, e.g., band gap, electron conductivity, transmittance,

Received 25 May 2023; Received in revised form 5 July 2023; Accepted 14 July 2023
Available online 25 September 2023

* Corresponding author, Lian-Huan Han, Tel: (86-592)18638012492, E-mail address: hanlianhuan@xmu.edu.cn.

* Corresponding author, Yun-Hua Liu, Tel: (86)13071265596, E-mail address: liuyh@mail.hust.edu.cn.

* Corresponding author, Dong-Ping Zhan, Tel: (86-592)2185797, E-mail address: dpzhan@xmu.edu.cn.

https://doi.org/10.13208/j.electrochem.3449

wettability, etc., and to fulfil the requirements of various industrial domains [8].

Great efforts have been made to fabricate SLG patterns. Physical methods can be classified into top-down and bottom-up categories [9]. The top-down methods are to remove the carbon atoms from pristine SLG wafer by the energy-beam techniques including the focused laser beam, electron beam, plasma beam, reactive ion beam, etc. [10]. The top-down methods can be realized by either direct writing or template forming combined with various lithography techniques. The bottom-up methods are to synthesize specially sized SLG on the patterned catalysts such as copper, nickel, platinum, gold, etc. [11−13]. The most advantage of physical methods lies that the crystalline structures of SLG are not destroyed. Consequently, the intrinsic properties of SLG are kept very well. Nevertheless, the physical properties of SLG, e.g., the band gap, can be regulated by the external physical field [14]. However, when the external physical field is dismissed, the band gap of SLG would go back to zero.

Comparing to physic methods, chemical micropatterning can change the crystalline structure and thus, change the physical and chemical properties of SLG [8]. Chemical adsorption [15] or doping [16] have been adopted to tune the SLG's properties by introducing the sp3-C defects. However, after thermal annealing, many of the functionalized SLG materials change back to be pristine due to the weak interaction between SLG and the adsorbates or dopants, e.g., van der Waals' force [17], adsorption bond [18], or even chemical bond [19]. To this, we developed an *in-situ* electrochemically induced radical addition reaction to functionalize SLG with high efficiency and stability [20,21]. Here we report that the functionalized SLG micropatterns have tuneable electron transport properties, making SLG to act as single-atomic-thickness resistor or rectifier, depending on the introduced sp^3-C defects density.

The electrochemical micropatterning and functionalization procedures of SLG are depicted as in Scheme 1. First, a thin-layer viscosifier (HMDS) was spin-coated on the SLG wafer to increase the adhesion between SLG and photoresist. Second, a thin layer of photoresist (AZ5214E) film was spin-coated on the substrate. Then, the photoresist film was exposed by the laser-beam direct-writing photolithography. Later on, the exposed photoresist was removed by tetramethylammonium hydroxide for several times and the aimed SLG micropattern array was obtained. After that, the obtained SLG micropattern array was immersed in an aqueous electrolyte containing 10 mmol·L^{-1} KBr and 10 mmol·L^{-1} H_2SO_4 to perform bromination addition reaction by cyclic voltammetry in a potential range from −0.75 to 1.2 V vs. Hg/Hg_2SO_4 reference electrode with a scan rate of 100 mV·s^{-1} for certain cycles (See Figure S1). Finally, the brominated SLG (SLGBr) micropatterns were obtained after removing the photoresist protection layer by rinsing with acetone and isopropanol.

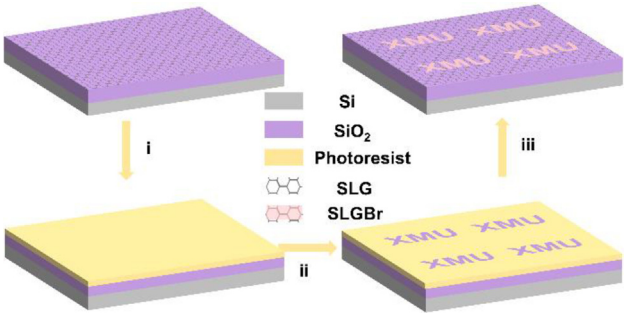

Scheme 1. Preparing processes of brominated SLG with patterns. (i) photoresist coating, (ii) Photolithography, (iii) electrochemical brominating.

As reported very recently by us, the functionalization of SLG is realized by the bromination addition reaction [20]. Because SLG is conductive enough to act as the working electrode, and bromide anions are oxidized to bromine radicals, which can react with SLG to form SLGBr. When SLG changes into SLGBr, the interfacial electrochemical reaction activity will be decreased because of the Faraday current keeping decreasing with the potential scanning going on. The colour of SLGBr micropatterns "XMU", the acronym of Xiamen University, was observed to differ from that of SLG by optical microscopy (Fig. 1a). The corresponding images of scanning electron microscopy (SEM) and scanning Raman microscopy (SRM) are shown in Fig. 1b and c, respectively. The clear boundaries between the SLG and SLGBr were also observed, indicating the different properties between them.

The Raman spectrum of the SLGBr region is much different from that of the SLG region (Fig. 1d). The pristine SLG has a G-peak at near 1586 cm^{-1} and a 2D peak at 2687 cm^{-1}. The 2D-peak is sharp and symmetrical, and the peak intensity is about 4 times larger than that of G-peak, indicating that the pristine SLG has a perfect lattice structure [22]. After the functionalization by bromination addition reaction, the newly observed D-peak (~1350 cm^{-1}) and D′-peak (~1620 cm^{-1}) represent the sp^3-C defects [23], indicating that the symmetry of the lattice is changed due to the formation of C-Br bond. Furthermore, the G-peak blue-shifted to 1597 cm^{-1} at the brominated region, and 2D peak blue-shifted

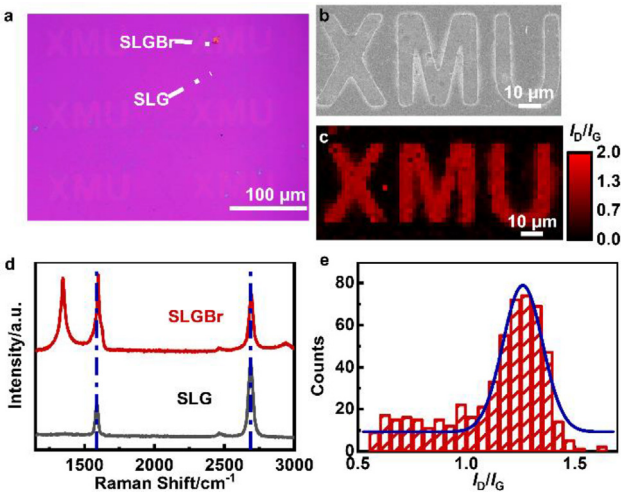

Fig. 1. The optical image (a) and SEM image (b) of patterned SLGBr with the "XMU" logo. (c) Raman ID/IG mapping image of the patterned SLGBr. (d) The corresponding Raman spectra of pristine SLG and SLGBr. (e) Statistical ID/IG histograms from the mapping image of (c).

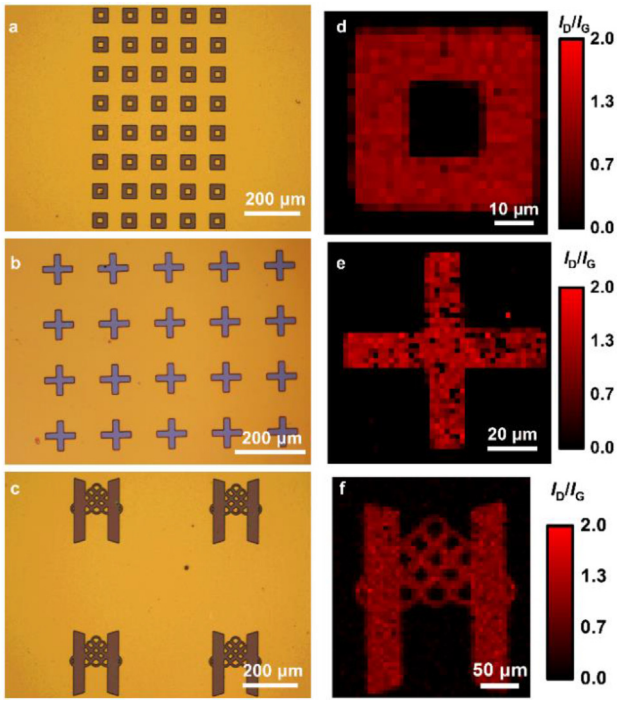

Fig. 2. (a–c) Optical images of SLG with photoresist patterns, including (a) square rings, (b) crosses and (c) H-type Chinese knot. (d–f) Corresponding Raman ID/IG mapping images of the SLGBr patterns.

to 2692 cm^{-1}, predicting that SLGBr is p-type doping [24], which is consistent with the strong electron absorption ability of bromine.

The intensity ratio (I_D/I_G) is usually adopted to characterize the defect density of graphene, that is, the ratio of the sp^3 to sp^2 bonding character. A higher the I_D/I_G ratio means a higher defect density [25]. The statistical analysis of SRM image gives a distribution of I_D/I_G ratio as shown in Fig. 1c. The I_D/I_G ratio in the "XMU" region is much higher than that in the remaining region, which indicates that photoresist micropattern can protect well the underlying graphene and let the bromination addition reaction selectively occur in the exposed area. The statistical I_D/I_G-ratio histogram was employed to analyzed the bromination degree of SLG. From Fig. 1e, I_D/I_G ranged from 0.5 to 1.5 with a mid-value about 1.2, suggesting that the bromination degree of SLGBr micropattern was pretty uniform.

To demonstrate the versatility and reliability of the method, SLGBr micropattern array such as square ring, cross and an H-type Chinese knot were fabricated. The optical microscopy images of the SLG micropatterns after laser-beam direct-writing photolithography are shown in Fig. 2a–c, and the relevant optical images of the SLGBr micropatterns are shown in Figure S2, indicating the clear SLG/SLGBr boundaries. The relevant I_D/I_G distribution of the SLGBr micropatterned SLG was characterized by the SRM as shown in Fig. 2d–f, indicating the uniform functionalization of bromination addition reaction.

We have demonstrated that the electron transport (i.e., electronic properties) and interfacial electron transfer (i.e., electrochemical properties) of functionalized SLG will be changed a lot from the pristine SLG [20]. To investigate the electron transport properties of SLGBr, we designed and fabricated the SLG-SLGBr interdigitated electrodes with a pair of Cr/Au belts as the current collectors (Scheme 2) to construct a field-effect transistor (FET), where the SLG electrode acts as the drain, the SLGBr acts as the source, and the Si/SiO_2 substrate acts as the gate. In order to investigate the characteristics of the devices, SLG electrodes and SLGBr electrodes were prepared simultaneously. The SLG electrodes exhibited resistance characteristics and p doping due to the residual photoresist (Figure S3a–3b), while the SLGBr electrodes with higher defect density showed semiconducting characteristics (Figure S3c–3d). Akin to chemical functionalization, electrochemically induced bromination addition introduced new sp^3 C-Br bond to SLG. Because of the asymmetric broken honeycomb structure, the bandgap of SLGBr rises, and a semimetal–semiconductor transition takes place in SLGBr.

Fig. 3a–c shows the I_{DS}-V_{DS} curves of the SLGBr/SLG FET with different bromination degree characterized by the statistical I_D/I_G mid-values from the SRM images of SLGBr. With the low bromination degree (I_D/I_G: 0.5 in Fig. 3a), the I_{DS}-V_{DS} curves show a typical electronic property of a resistor. The conductance, i.e., the slope of the I_{DS}-

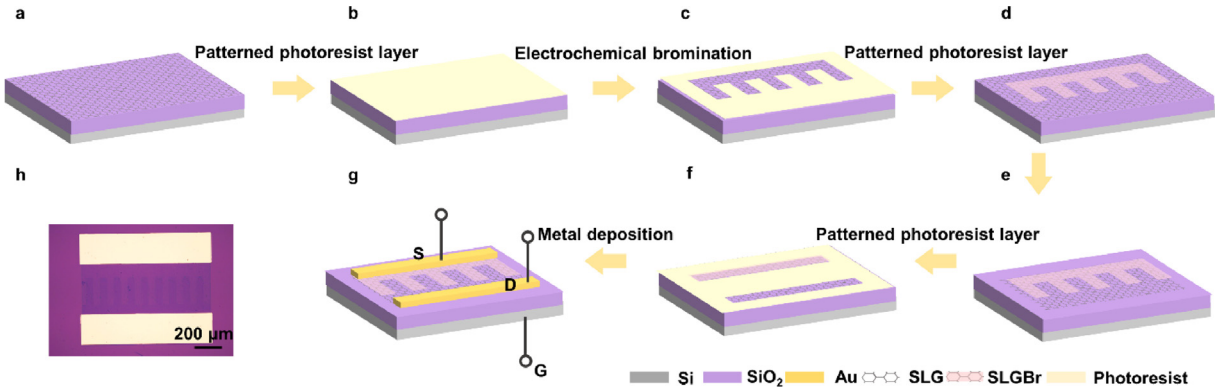

Scheme 2. (a–g) Preparing processes of the graphene Interdigitated Electrodes with designed SLGBr patterns. (h) The optical image of a typical Interdigitated Electrode with patterned SLGBr.

V_{DS} curves changes linearly with V_{GS} in a potential region [−50 V, +50 V], shown as the insert of Fig. 3a. The voltage-sensitive feature demonstrates the potential application of SLG into micro-varistor. With the higher bromination degree (I_D/I_G: 1.7 in Fig. 3b or 2.4 in Fig. 3c), the I_{DS}-V_{DS} curves were obviously different from those in Fig. 3a, presenting the characteristics of current rectification. The results show that the SLGBr will be changed into a semiconductor if the bromination degree becomes higher [20,26]. This result is similar to our previous study, but due to the low degree of bromination, the semiconductor characteristics are less significant than before [23]. We performed the electronic measurements of the FETs with different bromination degree and different V_{GS} bias, and the statistic relationship between the conductance (dI_{DS}/dV_{DS}) and the bromination degree (I_D/I_G) is shown in Fig. 3d. The critical I_D/I_G value between conductor and

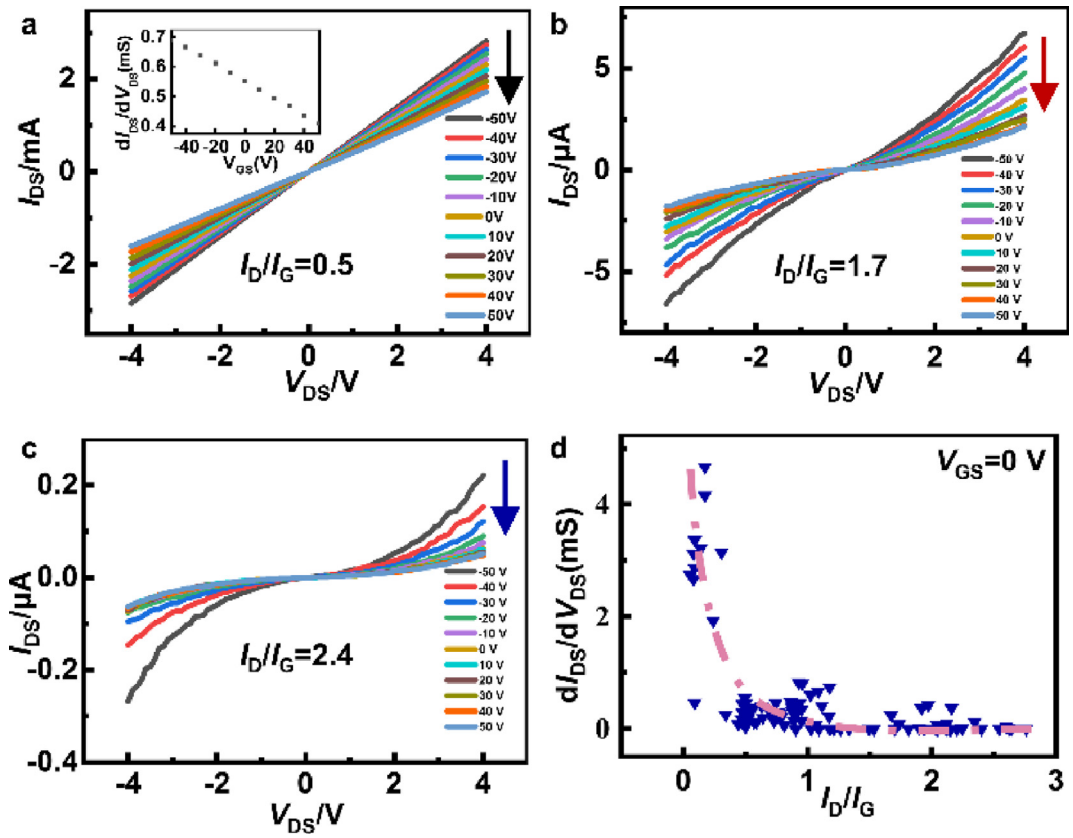

Fig. 3. (a–c) The I_{DS}-V_{DS} curves of the SLGBr Interdigitated Electrode when I_D/I_G values are 0.5 (a), 1.7 (b) and 2.4 (c). Inset in (a): the slope of the I_{DS}-V_{DS} curves changes with V_{GS}. (d) The statistic relationship curve between the bromination degree (I_D/I_G) and the conductance (dI_{DS}/dV_{DS}) at V_{GS} = 0 V.

semiconductor can be estimated as 0.6. The mechanism of the change of electron transport properties needs to be further studied in future.

In conclusion, laser beam direct-writing photolithography and electrochemically induced bromination addition reaction were adopted for the micropatterning and functionalization of SLG. We found that the brominating functionalization can tune the electron transport properties of SLG by controlling its bromination degree. The conductance of SLGBr keeps decreasing at low bromination degree. After a critical value, SLGBr will become a semiconductor. This work demonstrates the possibility for the fabrication of ultrathin microelectronic devices by SLG.

Acknowledgements

The financial support by the National Natural Science Foundation of China (21827802, 22202166, 22132003, 22021001) and the 111 Project (B08027, B17027) are appreciated. We thank Tan Kah Kee Innovation Laboratory for providing characterization services.

References

[1] Kaplan A, Yuan Z, Benck J D, Govind R A, Chu X S, Wang Q H, Strano M S. Current and future directions in electron transfer chemistry of graphene[J]. Chem. Soc. Rev., 2017, 46(15): 4530−4571.

[2] Morozov S V, Novoselov K S, Katsnelson M I, Schedin F, Elias D C, Jaszczak J A, Geim A K. Giant intrinsic carrier mobilities in graphene and its bilayer[J]. Phys. Rev. Lett., 2008, 100(1): 016602.

[3] Nair R R, Blake P, Grigorenko A N, Novoselov K S, Booth T J, Stauber T, Peres N M, Geim A K. Fine structure constant defines visual transparency of graphene[J]. Science, 2008, 320(5881): 1308.

[4] Nan H Y, Ni Z H, Wang J, Zafar Z, Shi Z X, Wang Y Y. The thermal stability of graphene in air investigated by Raman spectroscopy[J]. J. Raman Spectrosc., 2013, 44(7): 1018−1021.

[5] He Q Y, Wu S X, Yin Z Y, Zhang H. Graphene-based electronic sensors[J]. Chem. Sci., 2012, 3(6): 1764−1772.

[6] Biro L P, Nemes-Incze P, Lambin P. Graphene: nanoscale processing and recent applications[J]. Nanoscale, 2012, 4(6): 1824−1839.

[7] Schwierz F, Pezoldt J, Granzner R. Two-dimensional materials and their prospects in transistor electronics[J]. Nanoscale, 2015, 7(18): 8261−8283.

[8] Wei T, Bao L, Hauke F, Hirsch A. Recent advances in graphene patterning[J]. Chempluschem, 2020, 85(8): 1655−1668.

[9] Wei T, Hauke F, Hirsch A. Evolution of graphene patterning: from dimension regulation to molecular engineering[J]. Adv. Mater., 2021, 33(45): 2104060.

[10] Zheng Y Q, Wang H, Hou S F, Xia D Y. Lithographically defined graphene patterns[J]. Adv. Mater. Technol., 2017, 2(5): 1600237.

[11] Park J U, Nam S, Lee M S, Lieber C M. Synthesis of monolithic graphene-graphite integrated electronics[J]. Nat. Mater., 2011, 11(2): 120−125.

[12] Choi J K, Kwak J, Park S D, Yun H D, Kim S Y, Jung M, Kim S Y, Park K, Kang S, Kim S D, Park D Y, Lee D S, Hong S K, Shin H J, Kwon S Y. Growth of wrinkle-free graphene on texture-controlled platinum films and thermal-assisted transfer of large-scale patterned graphene[J]. ACS Nano, 2015, 9(1): 679−686.

[13] Zhou X B, Qi Y, Shi J P, Niu J J, Liu M X, Zhang G H, Li Q C, Zhang Z P, Hong M, Ji Q Q, Zhang Y, Liu Z F, Wu X S, Zhang Y F. Modulating the electronic properties of monolayer graphene using a periodic quasi-one-dimensional potential generated by hex-reconstructed Au(001)[J]. ACS Nano, 2016, 10(8): 7550−7557.

[14] Zhang Y, Tang T T, Girit C, Hao Z, Martin M C, Zettl A, Crommie M F, Shen Y R, Wang F. Direct observation of a widely tunable bandgap in bilayer graphene[J]. Nature, 2009, 459(7248): 820−823.

[15] Balog R, Jørgensen B, Nilsson L, Andersen M, Rienks E, Bianchi M, Fanetti M, Lægsgaard E, Baraldi A, Lizzit S, Sljivancanin Z, Besenbacher F, Hammer B, Pedersen T G, Hofmann P, Hornekær L. Bandgap opening in graphene induced by patterned hydrogen adsorption[J]. Nat. Mater., 2010, 9(4): 315−319.

[16] Wu J, Xie L M, Li Y G, Wang H L, Ouyang Y J, Guo J, Dai H J. Controlled chlorine plasma reaction for noninvasive graphene doping[J]. J. Am. Chem. Soc., 2011, 133(49): 19668−19671.

[17] Yavari F, Kritzinger C, Gaire C, Song L, Gulapalli H, Borca-Tasciuc T, Ajayan P M, Koratkar N. Tunable bandgap in graphene by the controlled adsorption of water molecules [J]. Small, 2010, 6(22): 2535−2538.

[18] Elias D C, Nair R R, Mohiuddin T M, Morozov S V, Blake P, Halsall M P, Ferrari A C, Boukhvalov D W, Katsnelson M I, Geim A K, Novoselov K S. Control of graphene's properties by reversible hydrogenation: evidence for graphane[J]. Science, 2009, 323(5914): 610−613.

[19] Wei T, Kohring M, Chen M, Yang S, Weber H B, Hauke F, Hirsch A. Highly efficient and reversible covalent patterning of graphene: 2D-management of chemical information[J]. Angew. Chem. Int. Ed. Engl., 2020, 59(14): 5602−5606.

[20] Zeng L P, Song W Y, Jin X F, He Q F, Han L H, Wu Y F, Lagrost C, Leroux Y, Hapiot P, Cao Y, Cheng J, Zhan D P. Electrochemical regulation of the band gap of single layer graphene: from semimetal to semiconductor[J]. Chem. Sci., 2023, 14(17): 4500−4505.

[21] Chen D H, Lin Z, Sartin M M, Huang T X, Liu J, Zhang Q G, Han L H, Li J F, Tian Z Q, Zhan D P. Photosynergetic electrochemical synthesis of graphene oxide[J]. J. Am. Chem. Soc., 2020, 142(14): 6516−6520.

[22] Zhong J H, Zhang J, Jin X, Liu J Y, Li Q, Li M H, Cai W, Wu D Y, Zhan D, Ren B. Quantitative correlation between defect density and heterogeneous electron transfer rate of single layer graphene[J]. J. Am. Chem. Soc., 2014, 136(47): 16609−16617.

[23] Ferrari A C, Basko D M. Raman spectroscopy as a versatile tool for studying the properties of graphene[J]. Nat. Nanotechnol., 2013, 8(4): 235−246.

[24] Li W, Li Y Q, Xu K. Facile, electrochemical chlorination of graphene from an aqueous nacl solution[J]. Nano Lett, 2021, 21(2): 1150−1155.

[25] Eckmann A, Felten A, Mishchenko A, Britnell L, Krupke R, Novoselov K S, Casiraghi C. Probing the nature of defects in graphene by Raman spectroscopy[J]. Nano Lett, 2012, 12(8): 3925−3930.

[26] Li B, Zhou L, Wu D, Peng H L, Yan K, Zhou Y, Liu Z F. Photochemical chlorination of graphene[J]. ACS Nano, 2011, 5(7): 5957−5961.

单层石墨烯微米尺度图案化和功能化：调控电子传输特性

崔苗苗[a]，韩联欢[a,b,*]，曾兰平[a]，郭佳瑶[a]，宋维英[a]，刘川[a]，吴元菲[a]，罗世翊[a]，刘云华[c,*]，詹东平[a,*]

[a]厦门大学化学化工学院化学系，固体表面物理化学国家重点实验室，电化学技术教育部工程研究中心，福建 厦门 361005

[b]厦门大学萨本栋微纳米科学与技术研究所机电工程系，福建 厦门 361005

[c]华中科技大学国家 CAD 支撑软件工程研究中心，湖北 武汉 430074

摘要

石墨烯具有优异的物理特性，如单原子厚度、极高的载流子迁移率等。然而，其零带隙的半金属特性限制了题在高性能场效应晶体管中的应用。为此，研究者们提出了石墨烯纳米化、外场诱导、掺杂以及化学图案化等策略，以调控其带隙宽度。但是，这些方法的可控性以及稳定性还需要进一步改善。在本研究中，我们提出采用电化学溴化并结合光刻图案化调控单层石墨烯的电子传输特性，通过这种方法，成功制备了图案化的溴化石墨烯（SLGBr）。进一步研究表明，单层石墨烯的电子传输性能可以通过溴化程度来调控。当溴化程度较小时，SLGBr 表现为电阻特性，且其电导随溴化程度增加而减小；当溴化程度增加到一定值时，SLGBr 表现为与半导体类似的特性。本研究将为全石墨烯器件的制备提供可行的技术路线，拓展其在微电子领域的应用。

关键词：石墨烯图案化；电子传输；电化学溴化；光刻；全石墨烯器件